

SUPPLEMENTARY TABLE

Supplementary Table 1. Crystallographic data collection and model refinement statistics for CC6/264.

ClyA variant CC6/264	Thr 2 – Val 302	Cys 6 – Val 302
Crystal form		
Space group	C222 ₁ (20)	C2 (5)
Unit cell dimensions a,b,c (Å)	94.92, 125.53, 186.79; $\alpha = \beta = \gamma = 90^\circ$	176.88, 48.44, 152.43; $\alpha = \gamma = 90^\circ, \beta = 102.34^\circ$
Data collection		
Wavelength (Å)	1.0	1.0
Resolution range (Å)	50.00 – 2.12	40.00 – 1.94
Unique reflections	63155 (9986)	85704 (12628)
Completeness (%)	99.5 (97.1)	91.0 (89.2)
R _{merge} (%)	6.4 (86.1)	8.0 (51.8)
I/σ	21.63 (3.10)	11.50 (2.55)
Wilson B factor (Å ²)	39.62	23.60
Model Statistics		
Refinement		
Resolution range (Å)	48.10 – 2.12	39.55 – 1.94
Reflections working/free sets	59151 / 3020	85693 / 2000
R _{work} /R _{free} (%)	18.51 / 23.08	17.60 / 21.79
RMS deviations		
Bonds (Å)	0.007	0.007
Angles (°)	0.888	0.903
Ramachandran plot		
Favoured (%)	99.19	99.48
Allowed (%)	0.81	0.52

SUPPLEMENTARY FIGURES

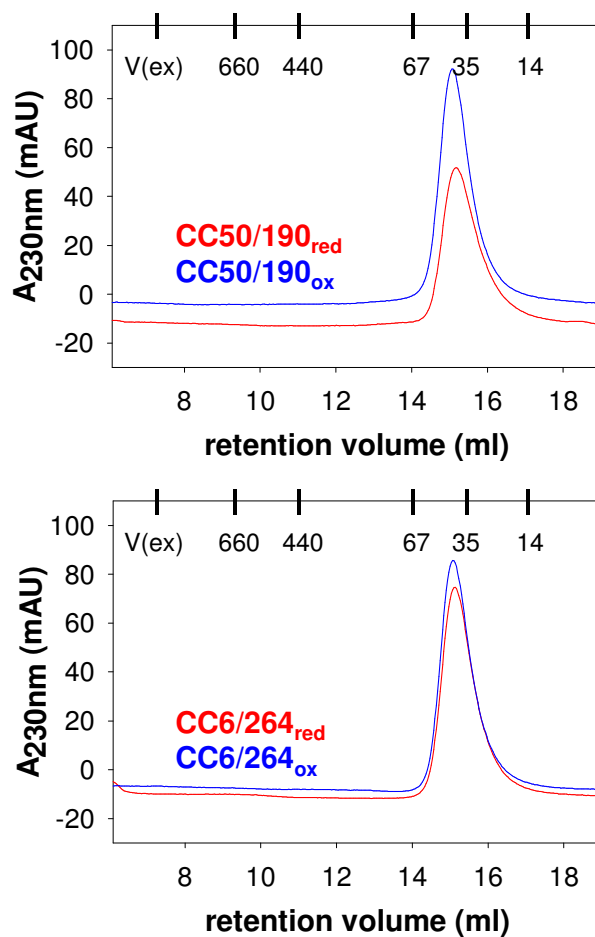


Figure S1. Gel filtration profiles of the reduced and oxidized ClyA variants CC50/190 and CC6/264 on a Superdex 200 10/300 column at pH 7.3, showing the monomeric state of the variants in both redox forms. Due to its elongated shape, the ClyA monomer (34.6 kDa for the (His)₆-tagged protein) shows a slightly increased apparent molecular mass of ~40 kDa in gel filtration experiments. The retention volumes of molecular mass standards (in kDa) and the exclusion volume (V_{ex}) are indicated.

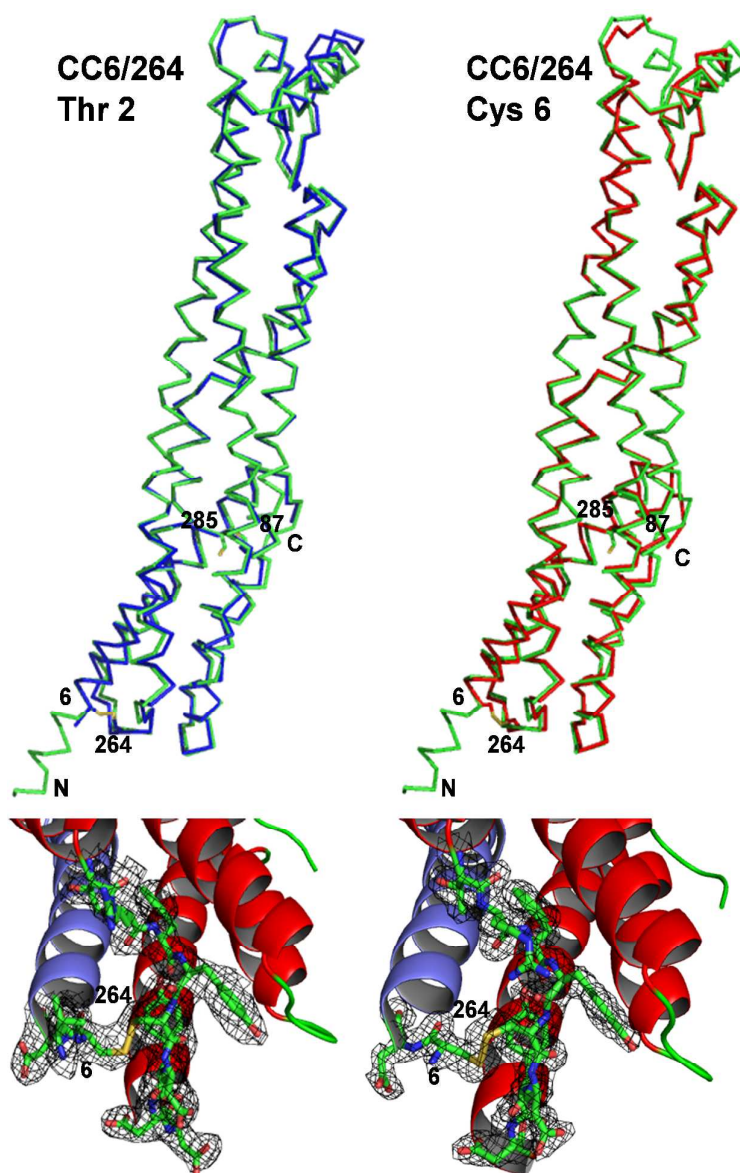


Figure S2: Ribbon representations of structural alignments of ClyA wt (pdb ID 1QOY) with chains from crystal structures of ClyA CC6/264 containing the artificial disulfide bond 6-S-S-264 (top). Structural alignments were performed using DaliLite. The positions of the wild type cysteines 87 and 285 and the engineered cysteines 6 and 264 are indicated. Left: 2.12 Å crystal structure of ClyA CC6/264 (2–303; blue) aligned with the 2.0 Å crystal structure of ClyA wt (green). Right: 1.94 Å crystal structure of ClyA CC6/264 (6–303; red) aligned with the 2.0 Å crystal structure of ClyA wt (green). Sections of both structures depicting the artificial disulfide bond (bottom). The electron density maps (contoured at 1.0 sigma) are shown for residues Val5–Asp7 (2–303, left) or Cys6 - Asp7 (6–303, right) and Thr260–Asp268. Figures were produced with PyMOL.

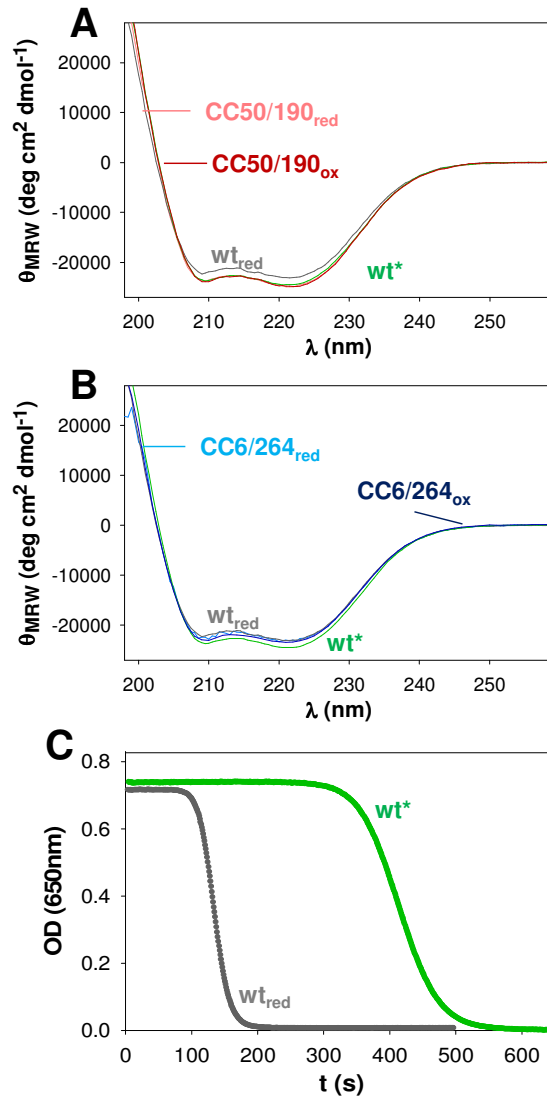


Figure S3: Far-UV CD spectra of ClyA and ClyA variants with the engineered disulfide bonds 50–190 and 6–264 are highly similar. Spectra of reduced wt ClyA, the cysteine-free pseudo wild type (w_{t^*}), and the variants CC50/190 and CC6/264 (8.9 μ M) at pH 7.3 and 22 °C are shown. A: Far-UV CD spectra of the reduced wt, w_{t^*} and the oxidized and reduced forms of the variant CC50/190. B: Far-UV CD spectra of wt, w_{t^*} and the oxidized and reduced forms of the variant CC6/264. C: Comparison of the hemolytic activity at 37 °C and pH 7.3 of reduced wt ClyA and w_{t^*} . Reactions were initiated by mixing horse erythrocytes at a density of 2×10^6 cells/ml with the respective ClyA protein (10 nM), and cell lysis was followed via the decrease in optical density at 650 nm.

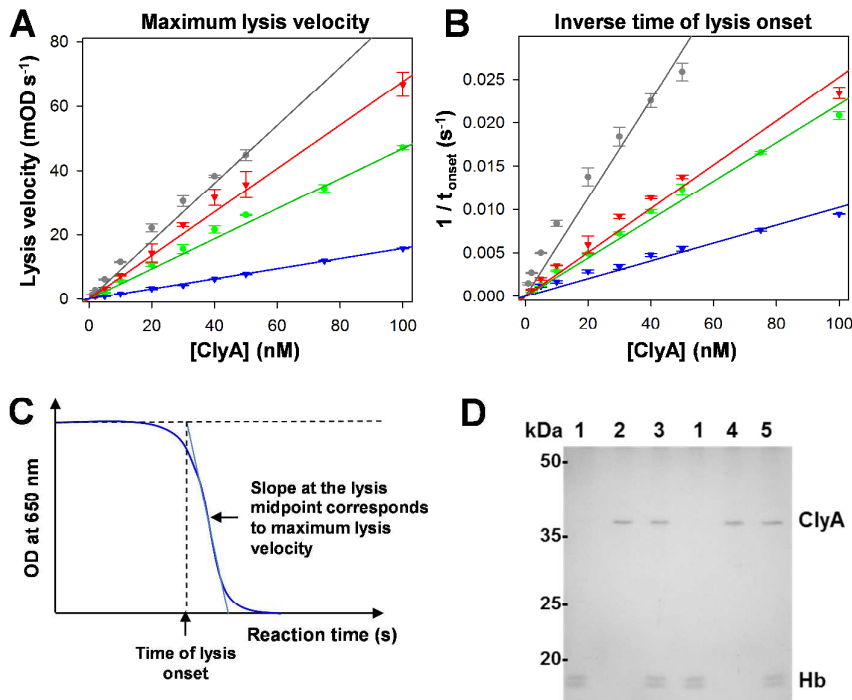


Figure S4: Evaluation of different parameters for quantifying the specific hemolytic activity of ClyA variants (see also Table S2). All measurements were performed at 37 °C , pH 7.3 with an initial density of 2×10^6 horse erythrocytes/ml, and initiated by adding varying concentrations (1–100 nM) of the respective ClyA monomer (gray: wt_{red}; green: wt*; red: CC50/190_{red}; blue: CC6/264_{red}). Error bars show the standard deviation from three independent measurements. The following parameters (see panel C for definitions) were plotted against the ClyA monomer concentrations: A: maximum lysis velocity; B: inverse time of lysis onset; C: Scheme defining the parameters for correlating hemolytic activity with ClyA concentration. D: The oxidized variants CC50/190_{ox} and CC6/264_{ox} (100 nM each) stay in the supernatant after incubation with erythrocytes (10^7 cells per ml) at 37 °C for 10 min and erythrocyte sedimentation by centrifugation. A Coomassie-stained SDS-polyacrylamide gel with samples (20 μ l each) of the following solutions is shown: (1) erythrocyte supernatant; (2) 100 nM CC50/190_{ox}; (3) CC50/190_{ox} in the supernatant after incubation with erythrocytes and centrifugation. (4) 100 nM CC6/264_{ox}; (5) CC6/264_{ox} in the supernatant after incubation with erythrocytes and centrifugation. Hb, released hemoglobin chains from a small fraction of lysed erythrocytes.

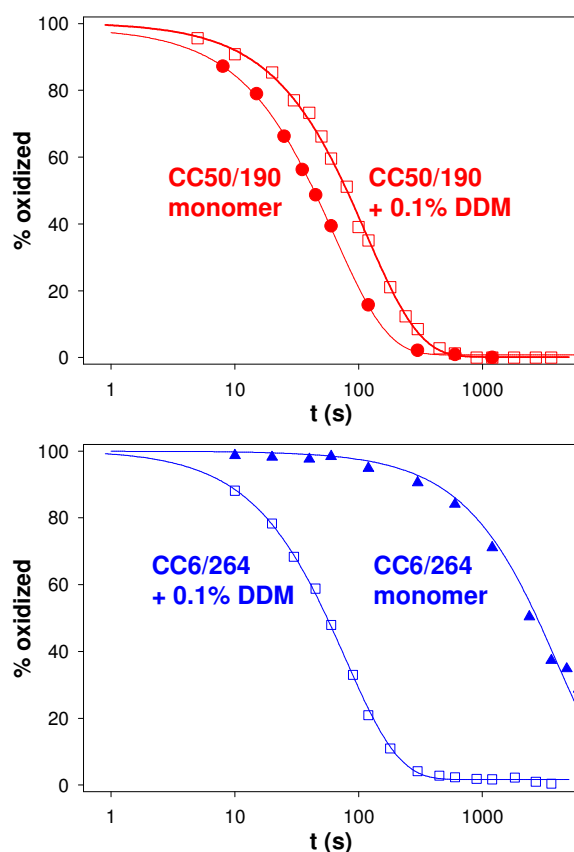


Figure S5: Comparison of the sensitivity for reduction by DTT of the oxidized ClyA variants CC50/190 (red, upper panel) and CC6/264 (blue, lower panel) in their monomeric state in the absence of DDM, and the DDM-induced intermediate state (I^{SS}). Reduction reactions were performed at 37 °C and pH 7.3 with 10 mM DTT. The reactions were acid-quenched after different times, and the oxidized and reduced proteins were separated by reversed-phase HPLC. The fraction of oxidized protein (determined with peak integration) was plotted against the reaction time and data were fitted to pseudo-first-order kinetics (solid lines). Closed circles: Reduction of oxidized monomers; open squares: Reduction of the I^{SS} state after incubation for 30 min in 0.1% DDM. The deduced second order rate constants are: CC50/190 monomer: $1.6 \pm 0.1 \text{ M}^{-1} \text{ s}^{-1}$; CC50/190 + 0.1% DDM (I^{SS} -state): $0.86 \pm 0.1 \text{ M}^{-1} \text{ s}^{-1}$; CC6/264 monomer: $2.4 \pm 0.1 \times 10^{-2} \text{ M}^{-1} \text{ s}^{-1}$; CC6/264 + 0.1% DDM (I^{SS} -state): $1.2 \pm 0.1 \text{ M}^{-1} \text{ s}^{-1}$. The results show that the engineered disulfide in the variant CC6/264 is deprotected 50-fold from reduction in the trapped intermediate I^{SS} , while the disulfide in the variant CC50/190 is protected 2-fold upon formation of I^{SS} .

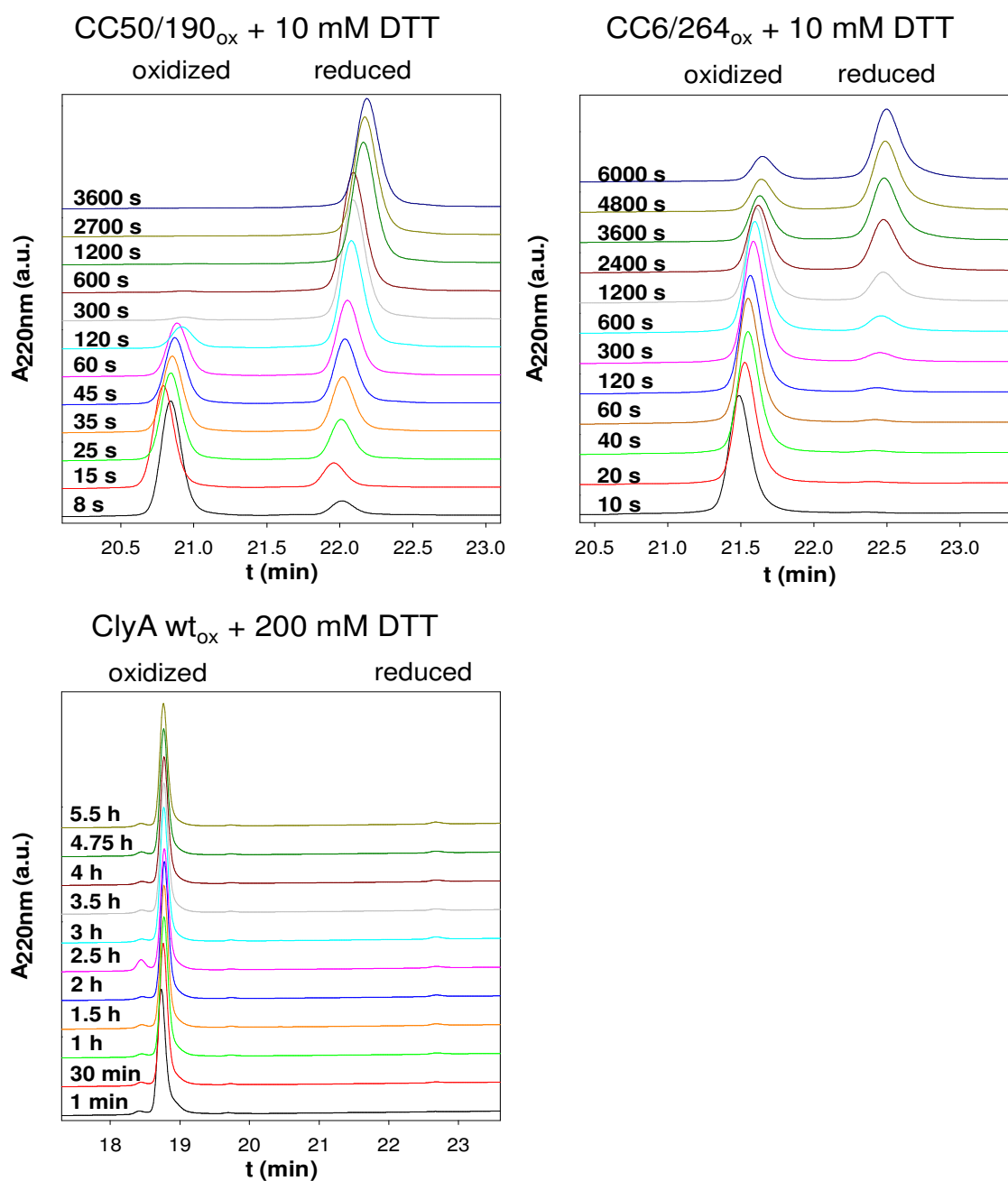


Figure S6: Reduction of oxidized ClyA wt and the oxidized variants CC50/190 and CC6/264 (5 μM each) with 200 mM DTT (wt) or 10 mM DTT (variants) at 37 $^{\circ}\text{C}$ and pH 7.3, and reversed-phase HPLC separation of oxidized and reduced protein after acid-quenching at different reaction times. Proteins were separated on a Zorbax 300SB C8 column (Agilent), eluted with a linear acetonitrile gradient (30–80% (v/v) in 0.1% trifluoroacetic acid) and detected via their absorbance at 220 nm.

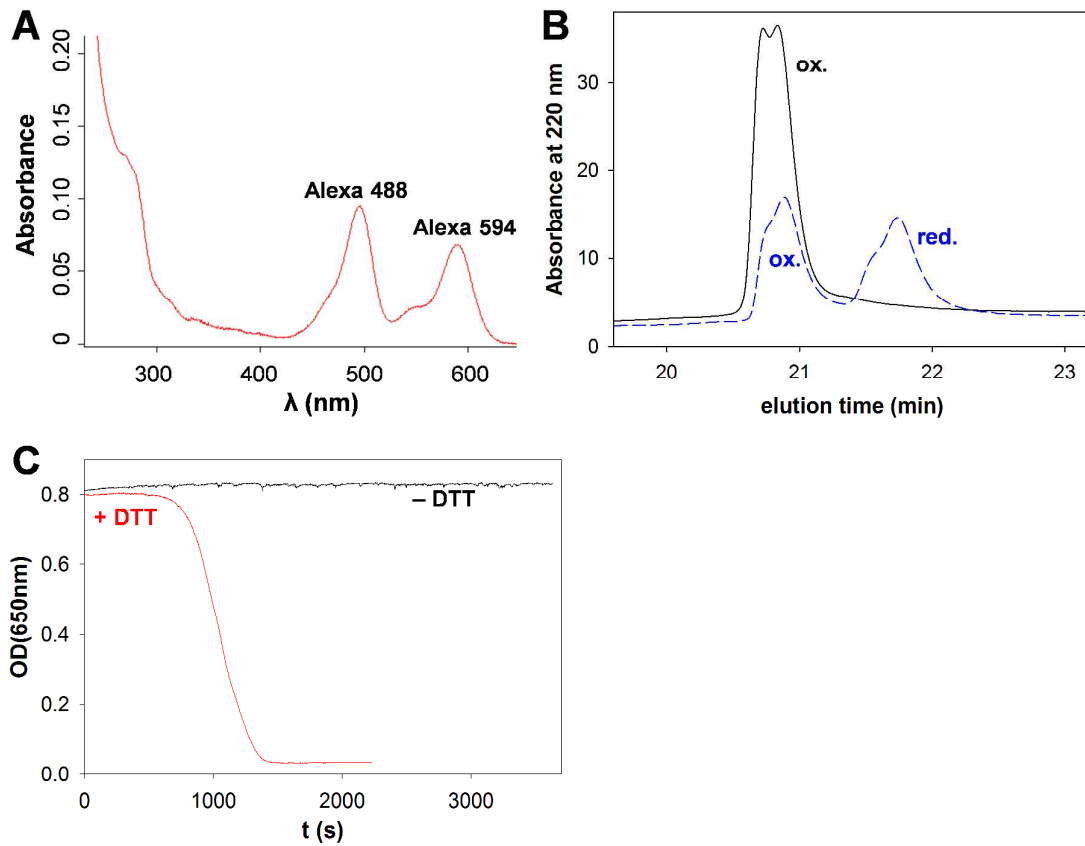


Figure S7: Verification of donor/acceptor labeling of the ClyA variant CC6/264 Q56C E252C and formation of the C6-C264 disulfide bond. A: Absorbance spectrum of the oxidized, double labeled protein after the final gel filtration step. Concentrations of protein-bound Alexa 488 and 594 were $1.30 \mu\text{M}$ and $0.74 \mu\text{M}$, respectively (see Materials and Methods for details). The protein concentration (average of Alexa 488 and Alexa 594 concentration) was $1.02 \mu\text{M}$. B: Reversed-phase HPLC profile of double labeled, oxidized ClyA CC6/264 Q56C E252C used in all single-molecule experiments (solid, black line). The dotted, blue line corresponds to a preparation where the second labeling step was performed with an excess of Alexa 594 over protein so that the cysteine pair C6/C264 also became partially labeled and only about 50% of the molecules could form the C6/C264 disulfide bond. The chromatogram shows that oxidized and reduced protein can be separated well under the HPLC conditions, and that the preparation of double labeled ClyA CC6/264 Q56C E252C (black line) used for single molecule experiments was oxidized quantitatively. C: Reduction of the disulfide bond C6/C264 by DTT regenerates hemolytic activity

of the donor/acceptor labeled variant CC6/264 Q56C E252C (+DTT, red line), while the disulfide-intact variant (-DTT, black line) lacks hemolytic activity. Horse erythrocytes (2×10^6 cells/ml) were mixed with 20 nM ClyA at 37 °C and pH 7.3, and the decrease in optical density at 650 nm as a consequence of erythrocyte lysis was recorded. The red hemolysis curve represents the reaction started by addition of 20 mM DTT to the erythrocyte suspension pre-incubated with oxidized, donor/acceptor labeled ClyA CC6/264 Q56C E252C.

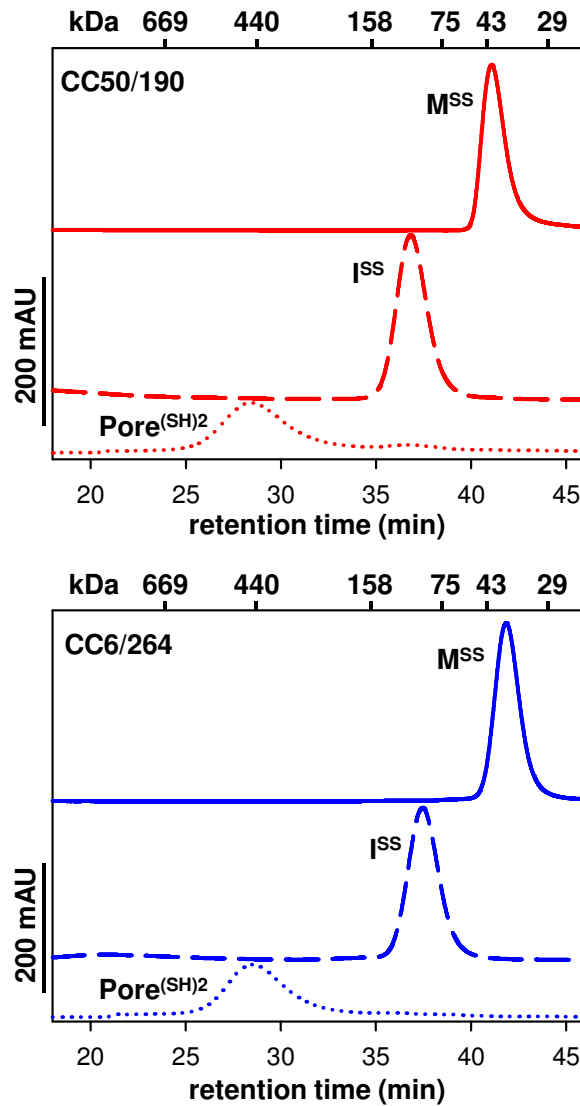


Figure S8: Size exclusion chromatography on Superdex 200 of the I^{SS} states (dashed lines) of ClyA CC50/190_{ox} (top panel, red lines) and CC6/264_{ox} (bottom, blue lines) at 22°C and pH 7.3. The I^{SS} states were populated by incubation of the oxidized variants in 0.1% DDM for 1.5 hours prior to chromatography in PBS buffer containing 0.1% DDM. As a control, gel filtration runs were also performed with the respective monomers (M^{SS} states, solid lines) in PBS without DDM, and with the assembled pore complexes of the reduced variants ($Pore^{(SH)2}$, dotted lines) in PBS, 0.1% DDM. The retention times of molecular mass standard proteins are indicated at the top of each panel. The I^{SS} states of both variants eluted at retention times expected for a ClyA monomer embedded in a DDM micelle (34 kDa + 70 kDa).

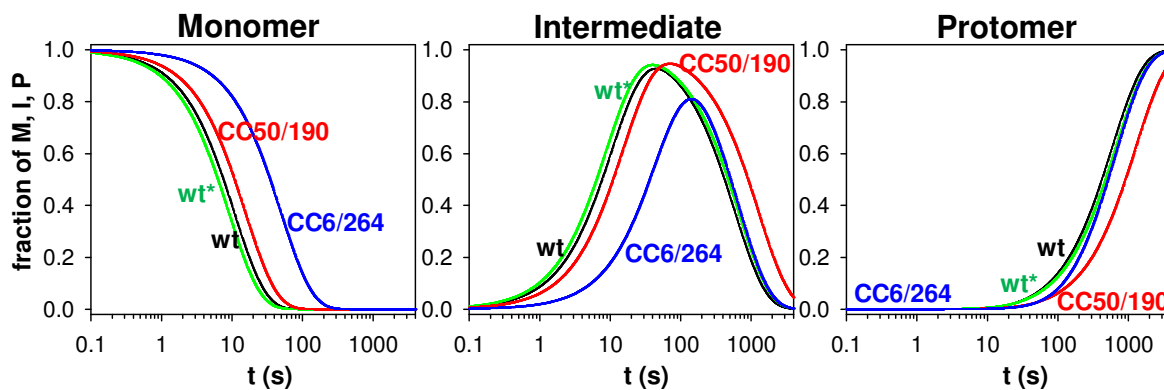


Figure S9: Simulation of the fractions of monomer, intermediate, and protomer of ClyA wt, wt* and the reduced variants CC50/190 and CC6/264 derived from the rate constants k_{MI} and k_{IP} that were obtained by ANS fluorescence measurements (cf. Figure 6 and Table 1). The intermediates of wt, wt*, and CC50/190 are maximally populated to more than 92%. The intermediate of CC6/264 is maximally populated to 81%.